Cross-Conjugated Poly(selenylene vinylene)s

Journal:	*Polymer Chemistry*
Manuscript ID	PY-ART-10-2018-001555.R1
Article Type:	Paper
Date Submitted by the Author:	14-Jan-2019
Complete List of Authors:	Zhang, Zhen; University of New Mexico, Chemistry and Chemical Biology Qin, Yang; University of New Mexico, Chemistry and Chemical Biology

Journal Name

ARTICLE

Cross-Conjugated Poly(selenylene vinylene)s

Zhen Zhang[a] and Yang Qin*[a]

Received 00th January 20xx,
Accepted 00th January 20xx

DOI: 10.1039/x0xx00000x

www.rsc.org/

Poly(selenylene vinylene) (PSV) is a close analog to the extensively studied poly(thienylene vinylene) (PTV) polymers, and possesses unique properties originating from the larger, more polarizable Se atoms. Currently, little is known about the structure-property relationships of PSV derivatives, caused by the lack of efficient synthetic methods that are capable of producing systematically varied polymer structures beyond the prototypical alkylated version. We report herein a facile synthetic methodology, combining acyclic diene metathesis (ADMET) and post-polymerization modification (PPM) techniques, for the preparation of a series of novel PSV polymers bearing different aromatic units cross-conjugated with the main-chain. Such structural modification allows fine-tuning of PSV electronic properties through main-chain/side-chain interactions and leads to fundamental understanding on the structure-property relationships of this class of unique materials. Our methodology is higly versatile in installing tailor-designed cross-conjugated side-chains to PSVs, as well as to other poly(arylene vinylene)s containing different heteroarenes.

Introduction

Since the discovery of metallic conductivity in doped polyacetylene that led to the Nobel Prize in 2001,[1-4] conjugated polymers (CPs) have evolved into a vast research field and been considered promising to revolutionize next-generation optoelectronics including organic superconductors, biological sensors, organic field-effect transistors, nonlinear optics, organic memory devices, thermoelectrics, and organic photovoltaics.[5-9] Poly(arylene vinylene)s (PAVs), with main-chains consisting of alternating aromatic and double bond moieties, are a prototypical class of CPs but have received much less attention than conventional polyaromatic systems. The insertion of a small-sized double bond between adjacent aromatic units can greatly release steric hindrance and lead to better main-chain coplanarity in PAVs.[10] So far, only two types of PAVs have been extensively studied, *i.e.*, poly(phenylene vinylene)s (PPVs) and poly(thienylene vinylene)s (PTVs). Compared with poly(para-phenylenes) (PPPs) and poly(3-alkylthiophene)s (P3ATs), comparably substituted PPVs and PTVs respectively possess reduced bandgaps and enhanced crystallinity.[11-12] Intriguingly, replacing the phenyl units in PPVs with thiophene as in PTVs generates new properties not found in PPVs, including the disappearance of fluorescence caused by the existence of a low-lying dark ^2A_g excited state[13] and activated singlet fission process[14] that is promising for overcoming the Shockley-Queisser limit[15] in solar cell efficiencies. Thus, introduction of other heteroarenes into the main-chain of PAVs may generate new materials with unexpected properties, and improve our fundamental understanding in previously under-explored areas of CP research.

Substituting thiophene with selenophene has recently become an attractive strategy in CP synthesis.[16-27] Compared with S atoms, the Se atom possesses larger atomic radius and polarizability, leading to less aromaticity in selenophene rings and enhanced electron accepting ability caused by σ*–π* interactions between the Se atom and ring double bonds.[28-29] As a result, Se-containing CPs typically display reduced optical bandgaps than their S analogs. The more polarizable Se atoms can also lead to stronger intermolecular interactions between neighboring polymer chains, resulting in a higher degree of overall rigidity and higher charge carrier mobility.[30] As the close analogue of PTVs, poly(selenylene vinylene) (PSV) has been rarely explored. The only examples of PSVs were prepared by Heeney et al. and Qin et al, through cross-coupling reactions and acyclic diene metathesis (ADMET) polymerization, respectively, and possess linear alkyl groups as the only side-chains.[31-33] These PSVs have shown reduced bandgaps and enhanced field-effect mobility when compared with similarly alkylated PTVs, and are thus promising materials for optoelectronic applications. However, current synthetic methodologies have not been able to diversify the PSV structures for a better understanding in structure-property relationships nor toward tailored adjustment of physical and electronic properties. Such ability of structural modification is intriguing as previously demonstrated in PTV derivatives by installing conjugated side-chains onto the main-chain thiophene moieties, which resulted in lower bandgaps, turn-on of fluorescence, and improved device performance.[34-36] Other

[a] *Department of Chemistry & Chemical Biology, University of New Mexico, Albuquerque, NM 87131, USA. E-mail: yangqin@unm.edu*

Electronic Supplementary Information (ESI) available: GC-MS spectra, SEC profiles, Raman spectra, CV voltammograms, and NMR spectra. See DOI: 10.1039/x0xx00000x

examples of using AMDET and PPM methodologies for the synthesis of substituted poly(phenylene vinylene) (PPV) and poly(fluorenylene vinylene) (PFV) derivatives have been reported previously.[37-43] In this account, we describe a facile synthetic methodology that first produces a novel brominated PSV polymer intermediate through ADMET, from which a series of cross-conjugated side-chains are then installed through cross-coupling reactions in a post-polymerization modification fashion.

Experimental

General Procedures

All reagents and solvents were used as received from Sigma-Aldrich or Alfa Aesar unless otherwise noted. 2,3,5-Tribromoselenophene and (5-(1,3-Dioxolan-2-yl)thiophen-2-yl)trimethylstannane were synthesized according to literature procedure.[33, 36] THF was distilled from Na/benzophenone prior to use. The 300.13 MHz ^{1}H and 75.48 MHz ^{13}C NMR spectra were recorded on a Bruker Avance III Solution 300 spectrometer. All solution ^{1}H and ^{13}C NMR spectra were referenced internally to solvent signals. Size exclusion chromatography (SEC) analyses were performed in chloroform with 0.5% (v/v) triethylamine (1 mL/min) using a Waters Breeze system equipped with a 2707 autosampler, a 1515 isocratic HPLC pump, and a 2414 refractive index detector. Two styragel columns (Polymer Laboratories; 5 µm Mix-C), which were kept in a column heater at 35 °C, were used for separation. The columns were calibrated with polystyrene standards (Varian). Ultraviolet–visible (UV–vis) absorption spectra were recorded on a Shimadzu UV-2401 PC spectrometer over a wavelength range of 240–900 nm. Raman spectra were obtained on a DXR SmartRaman spectrometer over a frequency range of 50.5–3350 cm^{-1}. Cyclic voltammetry was performed at 25 °C on a CH Instrument CHI604xD electrochemical analyzer using a glassy carbon working electrode, a platinum wire counter electrode, and a Ag/AgCl reference electrode calibrated using ferrocene redox couple (4.8 eV below vacuum). GC-MS measurements were performed on an Agilent 7820A system.

Solar Cell Fabrication and Testing

Polymer/$PC_{61}BM$ blend solutions were prepared by dissolving the polymer and $PC_{61}BM$ at predetermined weight ratios in chlorobenzene at a polymer concentration of 1 wt% and stirred at room temperature for 3-4 hours in a nitrogen glovebox (Innovative Technology, model PL-He-2GB, O_2 < 0.5 ppm, H_2O < 0.5 ppm). Solar cell devices were fabricated according to the following procedure: ITO-coated glass substrates (China Shenzhen Southern Glass Display Ltd.; 8 Ω/□) were cleaned by ultrasonication sequentially in detergent water, DI water, acetone and isopropyl alcohol, each for 15 min. These ITO-coated glasses were further treated by UV-ozone (PSD Series, Novascan) for 60 min before being transferred to a nitrogen glovebox (Innovative Technology, model PL-He-2GB, O_2 < 0.1 ppm, H_2O < 0.1 ppm) for MoO_3 deposition. MoO_3 (10 nm) was deposited using an Angstrom Engineering Amod deposition system at a base vacuum level of < 4×10^{-7} Torr. The PSVs/fullerene blend solution was first filtered through a 0.45 µm PTFE filter and spin-coated on top of the MoO_3 layer at 800 rpm for 30 s. Al (100 nm) was thermally evaporated through patterned shadow masks as cathodes, the size of the active areas is ca. 7.1 mm^2. Current-voltage (I-V) characteristics were measured using a Keithley 2400 source-measuring unit under simulated AM 1.5G irradiation (100 mW/cm^2) generated by a Xe arc-lamp based Newport 67005 150 W solar simulator equipped with an AM 1.5G filter. The light intensity was calibrated using a Newport thermopile detector (model 818P-010-12) equipped with a Newport 1916-C Optical Power Meter.

Synthetic Details

3-Bromoselenophene (1). CH_3COOH (10 mL), H_2O (26 mL) and zinc powder (11 g, 168.3 mmol) were charged into a round-bottom flask and heated up to 114 °C to reflux for 10 mins. 2, 3, 5-Tribromoselenophene (10.2 g, 27.7 mmol) was added into the flask after the reaction mixture was cooled down, and then the mixture was put back into the oil bath to reflux for 4 h. The reaction mixture was poured into water and extracted with diethyl ether (2 × 50 mL); the combined organic phase was then dried over anhydrous Na_2SO_4. After solvent removal under reduced pressure, the residue was further purified by vacuum distillation to give a colorless liquid (3.8 g, 66%). ^{1}H NMR (300.13 MHz, $CDCl_3$): δ (ppm) = 7.27 (dd, 1H), 7.87 (dd, 1H), δ (ppm) = 7.92 (dd, 1H). ^{13}C NMR (75.48 MHz, CDCl3): δ (ppm) = 110.66, 126.20, 131.39, 132.47.

3-Dodecylselenophene (2). In a two-neck flask, compound 1 (2.60 g, 12.4 mmol), Ni(dppp)Cl_2 (202 mg, 0.37 mmol) and THF (10 mL) were added. The mixture was kept in ice bath, then freshly prepared dodecylmagnesium bromide (25 mL, 18.6 mmol) was added. The reaction mixture was stirred at room temperature overnight. The reaction mixture was quenched with water and then extracted with diethyl ether (2×50 mL); the combined organic phase was then dried over anhydrous Na_2SO_4. After solvent removal under reduced pressure, the residue was further purified by column chromatography over silica gel to give a colorless liquid (1.66 g, 45 %). ^{1}H NMR (300.13 MHz, $CDCl_3$): δ (ppm) = 0.88 (t, 3H), 1.26 (m, 18H), 1.55~1.61 (m, 2H), δ (ppm) = 2.57~2.62 (t, 2H), 7.20~7.26 (dd, 1H), 7.53~7.54 (dd, 1H), 7.90~7.92 (dd, 1H). ^{13}C NMR (75.48 MHz, CDCl3): δ (ppm) = 14.11, 22.69, 29.33, 29.35, 29.47, 29.59, 29.64, 29.66, 29.67, 30.38, 31.91, 31.92, 123.74, 129.60, 131.42, 145.26.

2, 3, 5-Tribromo-4-dodecylselenophene (3). To a stirring solution of 3-dodecylselenophene (1.66 g, 5.53 mmol) in AcOH (1.6 mL) and H_2O (4.7 mL) was added Br_2 (2.3 mL, 44.3 mmol) slowly. The reaction mixture was covered with aluminum foil and kept at room temperature for 24 h. The reaction mixture was poured into Na_2SO_3 solution (50 mL) and extracted with diethyl ether (2 × 50 mL); the combined organic phase was then dried over anhydrous Na_2SO_4. After solvent removal under reduced pressure, the residue was further purified by column chromatography over silica gel to give the title compound as a clear liquid (1.65 g, 56 % yield). ^{1}H NMR (300 MHz, $CDCl_3$): δ (ppm) = 0.86~0.90 (t, 3H), 1.26 (m, 18H), 1.47~1.52 (m, 2H), 2.63~2.68 (t, 2H). ^{13}C NMR (75.48 MHz,

CDCl3): δ (ppm) = 14.17, 22.72, 28.41, 29.29, 29.37, 29.66, 31.94, 32.62, 110.59, 111.50, 117.25, 143.15.

3-Bromo-4-dodecyl-2,5-dipropenylselenophene (SV-Br). 2,3,5-Tribromo-4-dodecylselenophene (1.35 g, 2.52 mmol) and tri-n-butyl(1-propenyl) tin (1.67 g, 5.04 mmol) were charged into a pressure vessel. $Pd(PPh_3)_4$ (0.15 g, 0.13 mmol) and DMF (3 mL) were added into the vessel in an argon filled glovebox. The mixture was stirred at 110 °C for 24 h. The reaction mixture was poured into water and extracted with diethyl ether (2 × 50 mL); the combined organic phase was then dried over anhydrous Na_2SO_4. After solvent removal under reduced pressure, the residue was further purified by column chromatography over silica gel to give the title compound as a light yellow liquid (0.91 g, 79%). ^{1}H NMR (300 MHz, $CDCl_3$): δ (ppm) = 0.86~0.90 (t, 3H), 1.26 (m, 18H), 1.47 (m, 2H), 1.84~1.98 (d, 6H), 2.55~2.70 (t, 2H), 5.68~6.10 (m, 2H), 6.50~6.83 (d, 2H).

PSV-Br. In a two-neck round-bottom flask equipped with a condenser and rubber septum were added SV-Br (865 mg, 1.89 mmol) and CuI (36 mg, 0.19 mmol). Grubbs second-generation catalyst (16 mg, 0.019 mmol) in 5.5 mL of 1,2,4-trichlorobenzene was then added, and the reaction mixture was kept under dynamic vacuum while the condenser was cooled to 5 °C using a circulating chiller. The reaction mixture was gradually heated to 60 °C over 1 h and refluxed for 24 h. The reaction mixture was cooled down to room temperature, 16 mg of Grubbs second-generation catalyst in 3 mL of 1,2,4-trichlorobenzene was added, and the reaction mixture was refluxed at 60 °C under dynamic vacuum for another 24 h. Such a process was repeated for a total of five times, and the mixture was poured into Acetone (200 mL) to precipitate the polymer, which was purified by Soxhlet extraction with acetone, hexanes, and chloroform to give the title compound as a black solid (0.60 g, 79% yield). ^{1}H NMR (300 MHz, $CDCl_3$): δ (ppm) = 0.88 (t, 3H), 1.25 (m, 18H), 1.53 (m, 2H), 2.52 (t, 2H), 6.72 (m, 2H). ^{13}C NMR (125.75 MHz, $CDCl_3$): δ (ppm) = 14.16, 22.74, 29.75, 31.98, 117.71, 123.86, 138.61, 143.02. SEC ($CHCl_3$, 1 mL/min): M_n = 13.2 kDa, M_w = 39.7 kDa, $Đ$ = 3.0.

PSV-Th. PTV-Br (100 mg, 0.25 mmol) and tri-n-butyl(2-thienyl)tin (0.13 g, 0.35 mmol) were charged into a pressure vessel. $Pd(PPh_3)_4$ (57 mg, 0.05 mmol), DMF (2.5 mL), and toluene (2.5 mL) were added into the vessel in an argon-filled glovebox. The mixture was stirred at 110 °C for 24 h. PSV-Th was isolated by precipitation into Acetone and drying under high vacuum as a black solid (80 mg, 79%). ^{1}H NMR (300 MHz, $CDCl_3$): δ (ppm) = 0.87 (t, 3H), 1.23 (m, 20H), 2.49 (t, 2H), 6.95 (d, 2H), 7.14~7.59 (m, 3H). ^{13}C NMR (125.75 MHz, $CDCl_3$): δ (ppm) = 14.13, 22.70, 29.40, 29.68, 30.97, 31.92, 124.18, 126.32, 126.89, 128.03, 128.52, 129.99, 134.81, 144.74. SEC ($CHCl_3$, 1 mL/min): M_n = 11.4 kDa, M_w = 19.2 kDa, $Đ$ = 1.7.

PSV-ThCHO. PSV-Br (100 mg, 0.25 mmol) and (5-(1,3-dioxolan-2-yl)thiophen-2-yl)trimethylstannane (111 mg, 0.35 mmol) were charged into a pressure vessel. $Pd(PPh_3)_4$ (57.4 mg, 0.05 mmol), DMF (2.5 mL), and toluene (2.5 mL) were added into the vessel in an argon-filled golvebox. The mixture was stirred at 110 °C for 24 h. The reaction mixture was dried under high vacuum to get rid of the solvent, and the residue was used in next step without further purification. The residual polymer from the previous step, THF (25 mL), H_2O (5 mL), and HCl (0.5 mL) were added into a one-neck flask. The reaction mixture was stirred at room temperature for 24 h. **PSV-ThCHO** was isolated by precipitation into Acetone and drying under high vacuum as a black solid (64 mg, 59% yield). ^{1}H NMR (300 MHz, $CDCl_3$): δ (ppm) = 0.86 (t, 3H), 1.22 (m, 18H), 1.37 (m, 2H), 2.51 (t, 2H), 6.66 (d, 1H), 7.02 (d, 2H), 7.82 (d, 1H), 9.98 (s, 1H). ^{13}C NMR (125.75 MHz, $CDCl_3$): δ (ppm) = 14.12, 22.68, 28.77, 29.38, 29.66, 30.94, 31.90, 123.74, 124.86, 129.97, 136.11, 139.63, 140.00, 140.39, 144.36, 145.58, 147.53, 182.74, 182.92. SEC ($CHCl_3$, 1 mL/min): M_n = 12.1 kDa, M_w = 18.9 kDa, $Đ$ = 1.6.

PSV-ThCN. PSV-ThCHO (100 mg, 0.23 mmol) and methyl cyanoacetate (46 mg, 0.46 mmol) were charged into a pressure vessel. Triethylamine (93.5 mg, 0.92 mmol) and $CHCl_3$ (3 mL) were added into the vessel in an argon-filled glovebox. The mixture was stirred at room temperature for 24 h. After solvent removal under reduced pressure, the solid was dissolved in chloroform (0.5 mL) and then dropped into Acetone (100 mL) to precipitate the polymer as a black solid after drying under high vacuum (76 mg, 64%). ^{1}H NMR (300 MHz, $CDCl_3$): δ (ppm) = 0.85 (t, 3H), 1.21 (m, 20H), 2.53 (t, 2H), 3.93 (s, 3H), 6.70 (d, 1H), 7.09 (d, 2H), 7.88 (d, 1H), 8.36 (s, 1H). ^{13}C NMR (125.75 MHz, $CDCl_3$): δ (ppm) = 14.11, 22.66, 29.37, 29.68, 30.99, 31.90, 53.28, 98.83, 115.76, 123.84, 130.34, 136.68, 137.22, 146.40, 147.90, 163.16. SEC ($CHCl_3$, 1 mL/min): M_n = 13.1 kDa, M_w = 21.7 kDa, $Đ$ = 1.7.

Results and Discussion

Synthetic procedures of monomers and cross-conjugated PSVs are summarized in Scheme 1. The starting material, 2,3,5-tribromoselenophene, was prepared according to reported literature.[33] De-bromination at the 2- and 5-substitution positions through reduction reaction using metallic zinc in acetic acid led to 3-bromoselenophene (**1**). Nickel-catalysed Grignard cross-coupling reaction of **1** with n-

Scheme 1. Synthesis of Monomers and Polymers

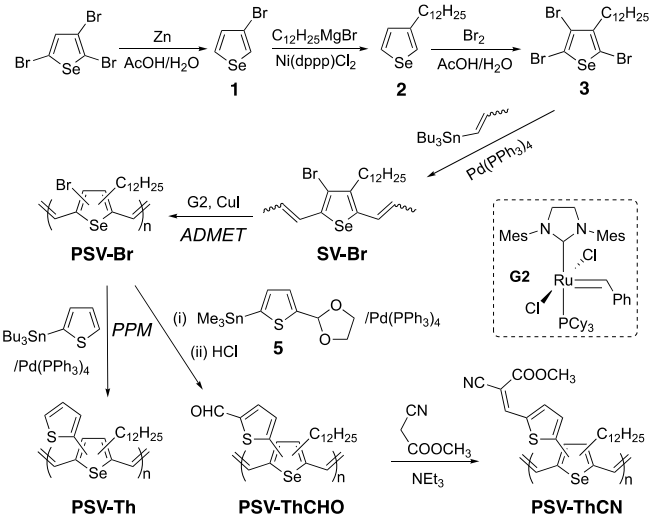

dodecylmagnesium bromide produced 3-dodecylselenophene (**2**). The long alkyl chain was chosen in order to ensure sufficient solubility of resulting PSV polymers without compromising efficient monomer synthesis and purification. Monomer **3** was obtained by bromination of **2** with an excess of bromine, which was subsequently subjected to Stille coupling reaction with 2 equivalents of tri-n-butyl(1-propenyl)tin to install propenyl groups selectively onto the 2- and 5- positions leading to monomer **SV-Br**. The selectivity of the reaction originates from the higher reactivity of the bromine atoms at the 2- and 5-positions, similar to that of thiophene derivatives we demonstrated previously,[36] and was confirmed by de-bromination reaction using isopropylmagnesium bromide followed by quenching with H_2O, leading to 3-dodecyl-2,5-dipropenylselenophene with similar NMR spectra as that of 3-decyl-2,5-dipropenylselenophene we prepared previously through a different route.[33] Further evidence came from GC-MS analyses of **SV-Br** as shown in Figure S1 (ESI). Three peaks are resolved in the GC trace of **SV-Br**, representing the different stereoisomers caused by *trans* and *cis* configurations of the double bonds at the asymmetric 2- and 5-postions, although we are unable to identify the relative abundance of each isomer due to the overlap of NMR signals. All three GC peaks gave exactly the same mass isotope patterns that match the calculated ones for **SV-Br**.

SV-Br was then subjected to acyclic diene metathesis (ADMET) polymerization toward the brominated intermediate poly(3-bromo-4-dodecylselenylene vinylene) (**PSV-Br**). ADMET is a versatile polymerization technique on diene monomers, which has been shown to tolerate a wide variety of functional groups and applied for the preparation of precision-substituted polyolefins and poly(arylene vinylene)s.[44-55] The ADMET polymerization of **SV-Br** was conducted in 1,2,4-trichlorobenzene (TCB) under dynamic vacuum at 60 °C in the presence of Grubbs second generation catalyst (G2) that was added in portions during 5 days in order to achieve high monomer conversion and polymer molecular weight. It's worth noting that the addition of 10 mol% CuI into the reaction mixture could greatly facilitate the polymerization rate, similar to the case of brominated PTV synthesis we demonstrated previously.[36] Such metathesis rate acceleration

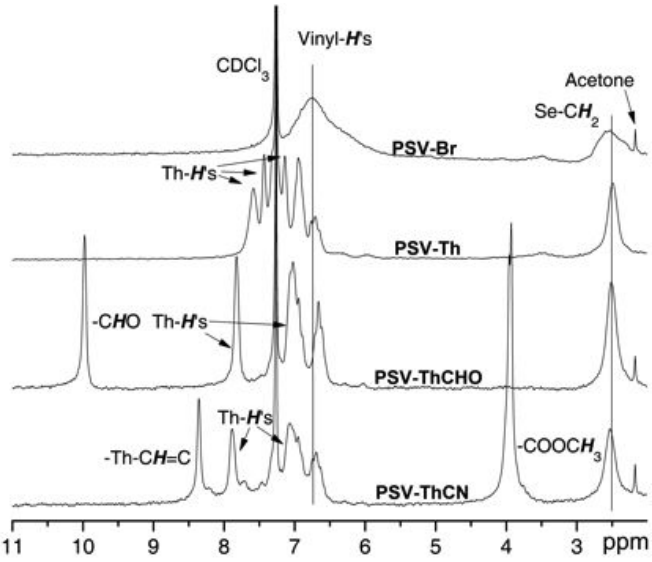

Figure 1. . ^{1}H NMR spectra of (top to bottom) **PSV-Br**, **PSV-Th**, **PSV-ThCHO**, and **PSV-ThCN** in $CDCl_3$.

effect by adding Lewis acids is likely caused by the phosphine sponge effect previously studied by Wagener et al. on olefin metathesis assisted by boron-containing compounds.[56] **PSV-Br** was isolated in high yields by precipitation into methanol and extensively purified by Soxhlet extractions as a black powder. Size-exclusion chromatography (SEC) measurements against polystyrene standards (Figure S2) gave a number-average molecular weight (M_n) of ca. 13.2 kDa, corresponding to an average degree of polymerization (DP) of ca. 33, and a dispersity index ($Đ$) of 3.0, consistent with the step-growth nature of ADMET polymerization. The absence of any visible signals from terminal propenyl groups in the ^{1}H NMR spectrum (Figure S5) of **PSV-Br** also suggests relatively high molecular weight of the polymer. The overall very broad signals indicate regio-random nature of **PSV-Br**, caused by the similar reactivity of propenyl groups at the 2- and 5-positions, similar to that of PTV derivatives we demonstrated previously.[36]

The unique feature of our synthetic method is the preparation of PSV polymers with a bromine substituent at every selenophene unit along the polymer backbone, which is incompatible with the previously employed Stille coupling

Table 1. Physical and Optical Properties of the PSV Polymers.

	M_n [a] (kDa)	$Đ$ [b]	DP [c]	$\lambda_{max, sol}$ [d] (nm)	$\lambda_{max, film}$ [e] (nm)	E_g [f] (eV)	HOMO [g] (eV)	LUMO [h] (eV)	E_g [i] (eV)
PSV-H	14.4	1.8	49	617	645	1.72 (1.58)	-4.62	-3.05	1.57
PSV-Br	13.2	3.0	33	646	653	1.54 (1.52)	-5.07	-3.32	1.75
PSV-Th	11.4	1.7	28	291, 646	305, 667	1.55 (1.49)	-4.96	-3.16	1.80
PSV-ThCHO	12.1	1.6	28	303, 648	309, 675	1.64 (1.45)	-5.03	-3.31	1.72
PSV-ThCN	12.8	1.8	25	369, 651	385, 680	1.43 (1.39)	-4.90	-3.70	1.20

[a] Number average molecular weight estimated from size exclusion chromatography (SEC) against polystyrene standards. [b] Dispersity index. [c] Average degree of polymerization estimated from M_n values. [d] Absorption maxima in chlorobenzene solution (ca. 10^{-5} M repeat unit). [e] Absorption maxima of polymer thin films on glass substrates. [f] Electronic bandgap estimated from optical absorption onsets, thin film data in parentheses. [g] Highest occupied molecular orbital energy estimated from cyclic voltammetry. [h] Lowest unoccupied molecular orbital energy estimated from cyclic voltammetry. [i] Electronic bandgap estimated from cyclic voltammetry.

polymerization, and can be conveniently used for the installation of functional side-chains through post-polymerization modification (PPM) reactions. As shown in Scheme 1, we have successfully attempted to install thienyl derivatives as the cross-conjugated side-chains, leading to **PSV-Th**, **PSV-ThCHO**, and **PSV-ThCN**, respectively containing simple thienyl, aldehyde functionalized thienyl, and thienyl groups bearing strongly electron-withdrawing cyanoester substituents. Conversions of such PPM reactions through Stille coupling on polymeric substrates are studied by ^{1}H NMR spectra of these PSVs as shown in Figure 1. Careful analyses and integrations of these NMR signals suggest close to quantitative, if not 100%, conversions of the PPM reactions. For example, by setting the integration value of the ^{1}H NMR signal from the CH_2 group directly attached to selenophene to 2.00, the integration values of signals from the aldehyde protons in **PSV-ThCHO** (Figure S14) and ester methyl protons in **PSV-ThCN** (Figure S16) are 1.01 and 3.00, respectively, comparing favourably with the theoretical values for quantitative substitution at 1.00 and 3.00. Noticeably, the post-polymerization modified PSVs displayed sharper and more resolved proton signals compared with that from **PSV-Br**, presumably due to less aggregation caused by the larger aromatic side-chains when compared with the single bromine atoms in **PSV-Br**. SEC traces of these cross-conjugated PSVs (Figure S2) show very similar profiles as that of **PSV-Br**, suggesting the absence of any significant polymer cross-linking or degradation during the PPM reactions. DPs of these cross-conjugated PSVs are estimated from the SEC M_n values, and the physical and electronic properties of all polymers, including **PSV-H** (i.e. poly(3-decylselenylene vinylene) we synthesized previously) are summarized in Table 1. The slightly different DPs among the cross-conjugated PSVs were likely caused by the different interactions between the functional groups and SEC column materials and/or different polymer aggregation behaviours in solution. It is also noticed that **PSV-Br** has a higher dispersity (*Đ*) than those of the cross-conjugated **PSV**s caused by high molecular weight shoulders in its SEC profile, which is presumably due to pronounced aggregation effects in this polymer induced by the smaller Br substituents when compared with larger aromatic side-chains in the other **PSV**s studied.

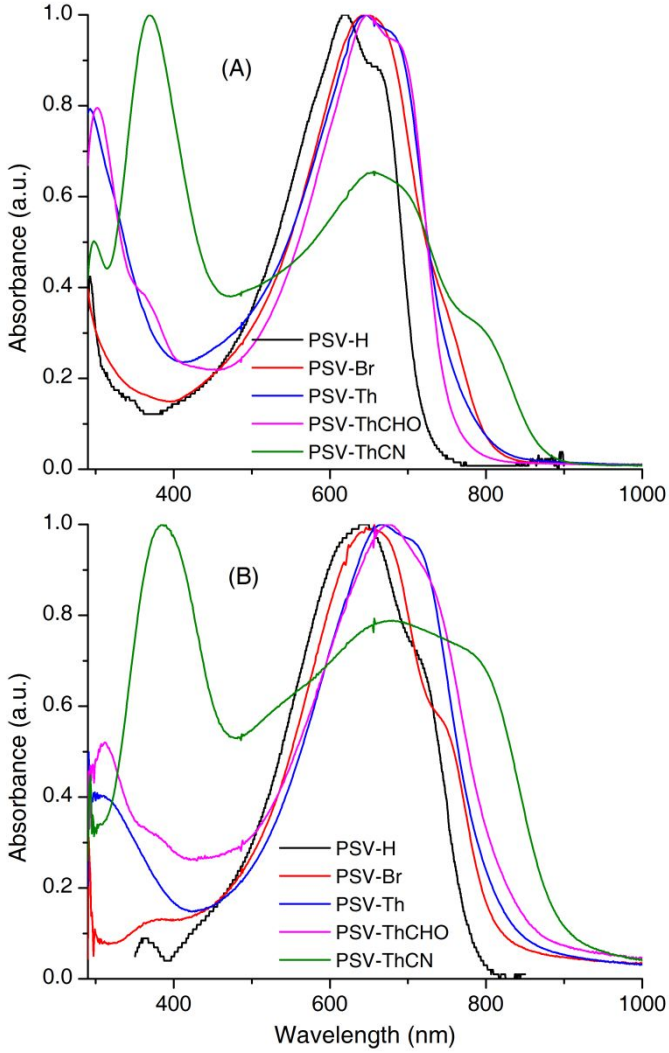

Figure 2. UV–vis absorption spectra of PSVs: (A) in chlorobenzene solutions (ca. 10^{-5} M r.p. units) and (B) as thin films spin-cast from chlorobenzene solutions onto glass substrates.

The newly prepared PSVs were first characterized by Raman spectroscopy in chlorobenzene solutions (ca. 10^{-5} M, Figure S3). All PSVs display similar Raman scattering profiles. The three major peaks from 1200 to 1600 cm^{-1} (insert, Figure S3), which have been previously assigned respectively to vinyl C–H bend, ring C=C stretch and vinyl C=C stretch,[57] are slightly red-shifted in cross-conjugated PSVs relative to those from **PSV-H**. This observation is consistent with the structures of cross-conjugated PSVs in which the electron withdrawing bromine atoms and cross-conjugated side-chains all effectively weaken the strengths of these chemical bonds through inductive and delocalization effects.

The optical properties of the PSVs were assessed by UV-vis absorption spectroscopy in both dilute chlorobenzene (CB) solutions and as thin films, and the results are summarized in Figure 2. Compared with **PSV-H**, **PSV-Br** and the cross-conjugated PSVs exhibit slightly red-shifted absorption maxima, likely resulted from the electron-withdrawing effect and the enlarged conjugated systems respectively, consistent with Raman scattering observation. For the cross-conjugated PSVs, the absorption signals emerge between 300 and 400 nm, which were assigned to the conjugated side-chains and that of PSV-ThCN is the most prominent at ca. 369 nm due to the cyanoester's strongly electron-withdrawing effect. The main absorption peaks of all PSVs in the red to near-IR regions are structured even in dilute solutions, which become slightly red-shifted and enhanced in thin films. We believe such phenomena are very similar to the case of PTV derivatives, and caused by aggregation effects even in very dilute solutions.[57-58] Such effect is further confirmed by variable temperature absorption studies as shown in Figure S4. The vibronic features and intramolecular charge transfer peak of **PSV-ThCN** all disappear upon heating to 120 °C, which, on the other hand, become more enhanced when the solutions are cooled down to 0 °C. A noticeable difference is that the vibronic features in the absorption peaks from brominated and cross-conjugated

PSVs are less pronounced than that from **PSV-H**, indicating less efficient π-π interactions between polymer chains and reduced main-chain coplanarity in these modified PSVs, which is presumably caused by the steric effects from large side-chains leading to more amorphous polymers and is consistent with ^{1}H NMR observations. The amorphous nature of these PSV polymers are further confirmed by differential scanning calorimetry (DSC) measurements as no thermal transition could be observed for all polymers except for **PSV-Br** at reduced scanning rate of 2°C/min, revealing only a glass transition temperature (T_g) at ca. 40 °C. All PSVs are relatively low bandgap materials displaying absorptions extending beyond ca. 800 nm in thin films, the bandgaps (Table 1) of which are respectively smaller than similarly functionalized PTV derivatives,[36] confirming the bandgap lowering effects from Se atom substitution. Intriguingly, **PSV-ThCN** displays a unique low-energy peak beyond 800 nm that is absent in other PSVs and results in a further reduced bandgap at ca. 1.43 eV in solution and ca. 1.39 eV in the solid state. We assign this structure-less low energy peak to main-chain to side-chain intramolecular charge transfer (ICT) electronic transition according to the similar phenomenon observed in cross-conjugated PTV derivatives.[36]

In order to corroborate with the optical properties observed, we performed cyclic voltammetry (CV) measurements on thin films of these PSVs in order to estimate their frontier orbital energies, as shown in Figure S6 and summarized in Table 1. All films showed quasi-reversible oxidation and reduction events, from the onsets of which we can respectively estimate the relative positions of their highest occupied molecular orbital (HOMO) and lowest unoccupied molecular orbital (LUMO). It is clearly seen that the HOMO and LUMO levels of brominated and cross-conjugated PSVs are all significantly lower than those of **PSV-H**, originating from the inductive and conjugation effects of these side-chains. **PSV-ThCN** displays the deepest LUMO level as expected from the strongly electron-withdrawing cyanoester groups but surprisingly the highest HOMO level among the modified PSVs, giving rise to the apparent smallest bandgap. This observation is also similar to those from cross-conjugated PTV derivatives.

In addition, we have performed density functional theory (DFT) calculations (B3LYP, 6-31G*) on oligomers containing three repeat units of **PSV-ThCN** with alkyl side-chains replaced with protons, and the results are shown in Figure S20. From the optimized structure, the main-chain of the oligomer is largely coplanar while the side-chain thiophene rings are all twisted out of plane with an average dihedral angle of 18°, which can potentially prevent close packing between polymer chains, leading to the observed amorphous nature of the polymer. The highest occupied molecular orbital (HOMO) is delocalized along the main-chain and the lowest unoccupied molecular orbital (LUMO) is localized on one of the side-chains, confirming the hypothesized main-chain to side-chain charge transfer interactions. Indeed, the simulated UV-vis absorption spectrum displays a low energy peak at 852 nm, corresponding to the HOMO to LUMO excitation, which agrees very well with the absorption spectroscopy measurements discussed earlier.

All PSVs studied here are non-emissive within the detection limit of our fluorescence spectrometer, and we are currently investigating in more detail the excitonic dynamics in these polymers by using ultra-fast transient absorption spectroscopy and will report any findings in future accounts.

Organic solar cell (OSC) devices have attracted significant research interests in recent years as alternative energy sources that possess unique properties including light weight and flexibility when compared with their inorganic counterparts.[59-62] We have fabricated OSC devices using the newly synthesized PSV polymers as electron donors in combination with phenyl-C61-butyric acid methyl ester (PCBM) as electron acceptor as the active layers. All devices adopt the basic ITO glass/MoO_3 (10 nm)/active layer (100 nm)/Al (80 nm) structures and were optimized by varying the donor/acceptor weight ratios, concentrations, spin coating conditions, and thermal annealing conditions. The results of optimized devices are summarized in Table S1. The open circuit voltage (V_{OC}) values, closely related to the energy differences between the donor HOMO and acceptor LUMO levels,[63] are consistent with the HOMO levels of polymers (Table 1), since **PSV-Br** has the deepest HOMO level of −5.07 eV, leading to the highest V_{OC} of 0.73 V. All devices suffer from relatively low short circuit current (J_{SC}) and fill factor (FF) values, leading to the best performing devices employing **PSV-Br** displaying power conversion efficiency at ca. 1.25%. Such relatively low performance is likely caused by the amorphous nature of these polymers, which can severely limit the conductivity of devices under light irradiation. Thus, our future efforts will be focused on improving polymer crystallinity by imparting regio-regularity and coplanarity of such cross-conjugated PSVs.

Conclusion

In summary, we have developed a facile methodology, by combining ADMET and PPM techniques, to prepare PSV derivatives containing cross-conjugated side-chains. A series of novel PSVs with thiophene-based substituents on selenophene rings along the polymer backbone were synthesized, which offered detailed structure-property relationship studies on these unique polymers for the first time. Our methodology is highly versatile in that differently functionalized cross-conjugated side-chains can be systematically installed to the common polymeric precursor **PSV-Br**; and is expected to be applicable to other poly(arylene vinylene) polymers containing various heteroarenes, thus opening great opportunities in this relatively less explored field in conjugated polymer synthesis.

Conflicts of interest

There are no conflicts to declare.

Acknowledgements

The authors would like to acknowledge NSF (DMR-1453083) for financial support for this research. NM EPSCoR (NSF Grant No. IIA-1301346) and USDA (NIFA 2015-38422-24059) are acknowledged for partially supporting the research.

Notes and references

1. H. Shirakawa; E. J. Louis; A. G. MacDiarmid; C. K. Chiang and A. J. Heeger, *J. Chem. Soc. Chem. Commun.,* 1977, 578.
2. H. Shirakawa, *Angew. Chem. Int. Ed.,* 2001, **40**, 2574.
3. A. G. MacDiarmid, *Angew. Chem. Int. Ed.,* 2001, **40**, 2581.
4. A. J. Heeger, *Angew. Chem. Int. Ed.,* 2001, **40**, 2591.
5. T. A. Skotheim and J. R. Reynolds, *Handbook of Conducting Polymers*. 3rd ed.; CRC Press: Boca Raton, 2007; Vol. 2 Volume Set.
6. W. R. Salaneck; K. Seki; A. Kahn and J.-J. Pireaus, *Conjugated Polymer and Molecular Interfaces - Science and Technology for Photonic and Optoelectronic Applications*. Marcel Dekker, Inc.: New York. Basel, 2002.
7. M. Leclerc and J.-F. Morin, *Design and Synthesis of Conjugated Polymers*. Wiley-VCH Verlag Gmbh & Co. KGaA: Weinheim, 2010.
8. B. Liu, *Conjugated Polymers for Biological and Biomedical Applications*. Wiley-VCH Verlag GmbH & Co. KGaA: Weinheim, Germany, 2018.
9. M. Knaapila, *Conjugated Polymers and Oligomers: Structural and Soft Matter Aspects (Materials and Energy)*. World Scientific Publishing: Singapore, 2018.
10. G. Koβmehl, *Ber. Bunsenges. Phys. Chem.,* 1979, **83**, 417.
11. T. Granier; E. L. Thomas; D. R. Gagnon; F. E. Karasz and R. W. Lenz, *J. Polym. Sci. Part B Polym. Phys.,* 1986, **24**, 2793.
12. M. L. Blohm; J. E. Pickett and P. C. Van Dort, *Macromolecules,* 1993, **26**, 2704.
13. E. Olejnik; B. Pandit; T. Basel; E. Lafalce; C.-X. Sheng; C. Zhang; X. Jiang and Z. V. Vardeny, *Phys. Rev. B,* 2012, **85**, 235201.
14. A. J. Musser; M. Al-Hashimi; M. Maiuri; D. Brida; M. Heeney; G. Cerullo; R. H. Friend and J. Clark, *J. Am. Chem. Soc.,* 2013, **135**, 12747.
15. W. Shockley and H. J. Queisser, *J. Appl. Phys.,* 1961, **32**, 510.
16. A. M. Ballantyne; L. Chen; J. Nelson; D. D. C. Bradley; Y. Astuti; A. Maurano; C. G. Shuttle; J. R. Durrant; M. Heeney; W. Duffy and I. McCulloch, *Adv. Mater.,* 2007, **19**, 4544.
17. M. Heeney; W. Zhang; D. J. Crouch; M. L. Chabinyc; S. Gordeyev; R. Hamilton; S. J. Higgins; I. McCulloch; P. J. Skabara; D. Sparrowe and S. Tierney, *Chem. Commun.,* 2007, 5061.
18. G. L. Gibson; T. M. McCormick and D. S. Seferos, *J. Am. Chem. Soc.,* 2011, **134**, 539.
19. H. A. Saadeh; L. Lu; F. He; J. E. Bullock; W. Wang; B. Carsten and L. Yu, *ACS Macro Lett.,* 2012, **1**, 361.
20. G. He; L. Kang; W. T. Delgado; O. Shynkaruk; M. J. Ferguson; R. McDonald and E. Rivard, *J. Am. Chem. Soc.,* 2013, **135**, 5360.
21. H. Yan; J. Hollinger; C. R. Bridges; G. R. McKeown; T. Al-Faouri and D. S. Seferos, *Chem. Mater.,* 2014, **26**, 4605.
22. R. L. Uy; L. Yan; W. Li and W. You, *Macromolecules,* 2014, **47**, 2289.
23. M. Jeffries-EL; B. M. Kobilka and B. J. Hale, *Macromolecules,* 2014, **47**, 7253.
24. A. K. Mahrok; E. I. Carrera; A. J. Tilley; S. Ye and D. S. Seferos, *Chem. Commun.,* 2015, **51**, 5475.
25. D. Gao; G. L. Gibson; J. Hollinger; P. Li and D. S. Seferos, *Polym. Chem.,* 2015, **6**, 3353.
26. S. M. Parke; M. P. Boone and E. Rivard, *Chem. Commun.,* 2016, **52**, 9485.
27. C.-H. Tsai; A. Fortney; Y. Qiu; R. R. Gil; D. Yaron; T. Kowalewski and K. J. T. Noonan, *J. Am. Chem. Soc.,* 2016, **138**, 6798.
28. A. Patra and M. Bendikov, Selenium- and Tellurium-Containing Organic π-Conjugated Oligomers and Polymers. In *The Chemistry of Organic Selenium and Tellurium Compounds*, Rappoport, Z.; Liebman, J. F.; Marek, I.; Patai, S., Eds. Wiley: 2012; Vol. 3, pp 523.
29. A. Patra and M. Bendikov, *J. Mater. Chem.,* 2010, **20**, 422.
30. K. Takimiya; Y. Kunugi; Y. Konda; N. Niihara and T. Otsubo, *J. Am. Chem. Soc.,* 2004, **126**, 5084.
31. M. Al-Hashimi; M. A. Baklar; F. Colleaux; S. E. Watkins; T. D. Anthopoulos; N. Stingelin and M. Heeney, *Macromolecules,* 2011, **44**, 5194.
32. M. Al-Hashimi; Y. Han; J. Smith; H. S. Bazzi; S. Y. A. Alqaradawi; S. E. Watkins; T. D. Anthopoulos and M. Heeney, *Chem. Sci.,* 2016, **7**, 1093.
33. Z. Zhang and Y. Qin, *ACS Macro Lett.,* 2015, **4**, 679.
34. L. Huo; T. L. Chen; Y. Zhou; J. Hou; H.-Y. Chen; Y. Yang and Y. Li, *Macromolecules,* 2009, **42**, 4377.
35. Y. Jiang; Q. Peng; X. Gao; Z. Shuai; Y. Niu and S. H. Lin, *J. Mater. Chem.,* 2012, **22**, 4491.
36. Z. Zhang and Y. Qin, *Macromolecules,* 2016, **49**, 3318.
37. E. Thorn-Csanyi and P. Kraxner, *Macromol. Rapid Commun.,* 1995, **16**, 147.
38. K. Nomura; H. Morimoto; Y. Imanishi; Z. Ramhani and Y. Geerts, *J. Polym. Sci. Part A Polym. Chem.,* 2001, **39**, 2463.
39. K. Nomura; Y. Miyamoto; H. Morimoto and Y. Geerts, *J. Polym. Sci. Part A Polym. Chem.,* 2005, **43**, 6166.
40. K. Nomura; N. Yamamoto; R. Ito; M. Fujiki and Y. Geerts, *Macromolecules,* 2008, **41**, 4245.
41. N. Yamamoto; R. Ito; Y. Geerts and K. Nomura, *Macromolecules,* 2009, **42**, 5104.
42. T. Miyashita and K. Nomura, *Macromolecules,* 2016, **49**, 518.
43. H. Weychardt and H. Plenio, *Organometallics,* 2008, **27**, 1479.
44. E. B. Berda and K. B. Wagener, *Macromolecules,* 2008, **41**, 5116.
45. G. V. Shultz; L. N. Zakharov and D. R. Tyler, *Macromolecules,* 2008, **41**, 5555.
46. G. V. Shultz; J. M. Zemke and D. R. Tyler, *Macromolecules,* 2009, **42**, 7644.
47. Y. Qin and M. A. Hillmyer, *Macromolecules,* 2009, **42**, 6429.
48. B. S. Aitken; M. Lee; M. T. Hunley; H. W. Gibson and K. B. Wagener, *Macromolecules,* 2010, **43**, 1699.
49. P. A. Delgado; D. Y. Liu; Z. Kean and K. B. Wagener, *Macromolecules,* 2011, **44**, 9529.
50. K. L. Opper and K. B. Wagener, *J. Polym. Sci. A. Polym. Chem.,* 2011, **49**, 821.
51. J. C. Speros; B. D. Paulsen; B. S. Slowinski; C. D. Frisbie and M. A. Hillmyer, *ACS Macro Lett.,* 2012, **1**, 986.
52. U. H. F. Bunz; D. Mäker and M. Porz, *Macromol. Rapid Commun.,* 2012, **33**, 886.
53. J. C. Speros; B. D. Paulsen; S. P. White; Y. Wu; E. A. Jackson; B. S. Slowinski; C. D. Frisbie and M. A. Hillmyer, *Macromolecules,* 2012, **45**, 2190.
54. J. C. Speros; H. Martinez; B. D. Paulsen; S. P. White; A. D. Bonifas; P. C. Goff; C. D. Frisbie and M. A. Hillmyer, *Macromolecules,* 2013, **46**, 5184.
55. L. C. da Silva; G. Rojas; M. D. Schulz and K. B. Wagener, *Prog. Polym. Sci.,* 2017, **69**, 79.
56. C. Simocko and K. B. Wagener, *Organometallics,* 2013, **32**, 2513.
57. J. Gao; A. K. Thomas; J. Yang; C. Aldaz; G. Yang; Y. Qin and J. K. Grey, *J. Phys. Chem. C,* 2015, **119**, 8980.

58. A. V. Gavrilenko; T. D. Matos; C. E. Bonner; S.-S. Sun; C. Zhang and V. I. Gavrilenko, *J. Phys. Chem. C,* 2008, **112**, 7908.
59. M. Jørgensen; J. E. Carlé; R. R. Søndergaard; M. Lauritzen; N. A. Dagnæs-Hansen; S. L. Byskov; T. R. Andersen; T. T. Larsen-Olsen; A. P. L. Böttiger; B. Andreasen; L. Fu; L. Zuo; Y. Liu; E. Bundgaard; X. Zhan; H. Chen and F. C. Krebs, *Sol. Energy Mater. Sol. Cells,* 2013, **119**, 84.
60. F. C. Krebs; N. Espinosa; M. Hösel; R. R. Søndergaard and M. Jørgensen, *Adv. Mater.,* 2014, **26**, 29.
61. S. Li; L. Ye; W. Zhao; H. Yan; B. Yang; D. Liu; W. Li; H. Ade and J. Hou, *J. Am. Chem. Soc.,* 2018, **140**, 7159.
62. L. Meng; Y. Zhang; X. Wan; C. Li; X. Zhang; Y. Wang; X. Ke; Z. Xiao; L. Ding; R. Xia; H.-L. Yip; Y. Cao and Y. Chen, *Science,* 2018, **361**, 1094.
63. B. Qi and J. Wang, *J. Mater. Chem.,* 2012, **22**, 24315.

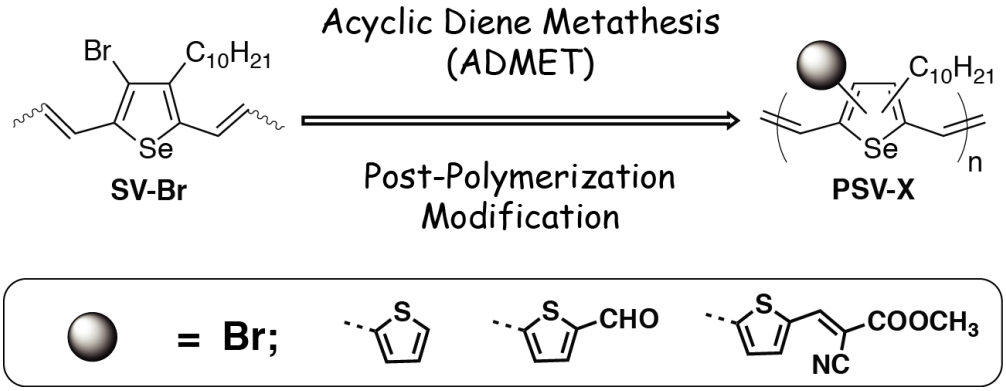
Acyclic Diene Metathesis
(ADMET)
Post-Polymerization
Modification
Br
$C_{10}H_{21}$
Se
SV-Br
$C_{10}H_{21}$
Se
n
PSV-X
= Br;
S
S
CHO
S
COOCH3
NC